Progress In Electromagnetics Research M, Vol. 47, 37–44, 2016

Low-Power Far Field Nanonewton Optical Force Trapping Based on Far-Field Nanofocusing Plasmonic Lens

Pengfei Cao[1, 2, *] and Lin Cheng[1]

Abstract—In this article, we study the far-field trapping behavior of dielectric nanospheres with diameter of 200 nm by utilizing a plasmon enhanced far-field nanofocusing lens. Based on our high effect nanofocusing circular plasmonic lens, such a far-field plasmonic trap is constituted by illuminating with a laser to form a sharper focus (subwavelength) due to a constructive interference of cylindrical surface plasmon wave. The nanoparticles can be steadily trapped in the far-field focal region (4.4λ) with an optical force to nanonewton (-4.76 nN) order, and the required optical power is less than 0.5 W. Compared with other surface plasmon tweezers, the proposed far-field plasmonic tweezers can not only avoid physical contact with the trapped particles to prevent contamination and reduce thermal damage effects due to metal absorption, but also enable the easy trapping and manipulation of nanosize dielectric particles owing to nanonewton scale forces.

1. INTRODUCTION

Since optical tweezers were first introduced by Ashkin in 1970 [1] to trap dielectric beads in lower-refractive-index media, the optical trap has become an indispensable tool for manipulating micrometer-scale objects without any mechanical contact, particularly in the biosciences [2–6]. Unfortunately, traditional far-field optical traps face trapping size limitations based on the diffraction limits; in particular, considering an object of radius r, the trapping efficiency drops rapidly (following $\sim r^3$ law). Therefore, nanoscale objects escape easily because their physical sizes are smaller than the potential well of trap. One can overcome this problem by increasing the optical power to strengthen the trap. However, bio-samples typically undergo quick photo damage at high optical powers.

To overcome diffraction-limited problem, near-field optical manipulation techniques have been developed; these techniques exploit the strong optical forces that can be generated in the near field of surface plasmon (SP) structures [7–19]. Metallic plasmonic nanostructures allow deep subwavelength concentration of the light and resonant enhancement of the optical field intensity. It results in the generation of a strong gradient optical force field, which is conducive to obtain strong optical traps. Several studies [20–28] have recently demonstrated that the plasmonic optical trapping requires illumination power to remain below 10 mW. However, there are some drawbacks. First, because of the evanescent nature of the SP, the SP tweezers can only be used for near-field trapping, which means that the trapped particles will likely have physical contact with the tweezers structures and hence lead to contamination. Second, since it is near-field trapping, near-field thermal effects caused by the absorption of SPs in metal nanostructures cannot be neglected. The thermal effects can limit trapping stability [29] and even cause thermal damage to bio-samples. Recent progress on far-field plasmonic optical trapping [30] can overcome these drawbacks. Unfortunately, the force range available to far-field plasmonic tweezers limits their applicability, with trapping forces usually spanning from subpiconewtons to ~ 1 pN. This scale is compatible with the forces that individual molecular machines generate [31], but

Received 21 January 2016, Accepted 4 March 2016, Scheduled 20 March 2016

* Corresponding author: Pengfei Cao (caopf@lzu.edu.cn).

[1] School of Information Science and Engineering, Lanzhou University, Tianshui south road 222, Lanzhou 730000, China. [2] Kirchhoff-Institute for Physics, Im Neuenheimer Feld 227, Heidelberg 69120, Germany.

the mechanical characterization of macromolecules, their assemblies or more complex cellular processes require much larger forces. For example, the forces of protein unfolding, cell adhesion and contraction may be at a nanonewton scale or more, which is beyond the capabilities of this far-field plasmonic optical trap [31, 32]. Therefore, the problem is how to create efficient far-field plasmonic trapping that provides a strong optical force with low illumination power.

Here we present a new approach to create a low power far-field nanonewton plasmonic optical trapping, in which a dielectric surface grating on the circular plasmonic lens [33] is employed to generate a strong subdiffraction-limit focus. This tight subdiffraction-limit focus generates a strong field gradient and enables three-dimensional (3D) optical trapping of nano-sized particles, as illustrated in Fig. 1(a). Compared to the other far-field plasmonic optical tweezers with weak trapping forces, the trap force created by our plasmonic lens can not only keep all the advantages of other far-field plasmonic optical tweezers, such as avoiding physical contact with trapped particles, but also achieve nanonewton scale in the far field due to high focusing efficiency (733% [33]), which can be used to complex cellular processes [31, 32].

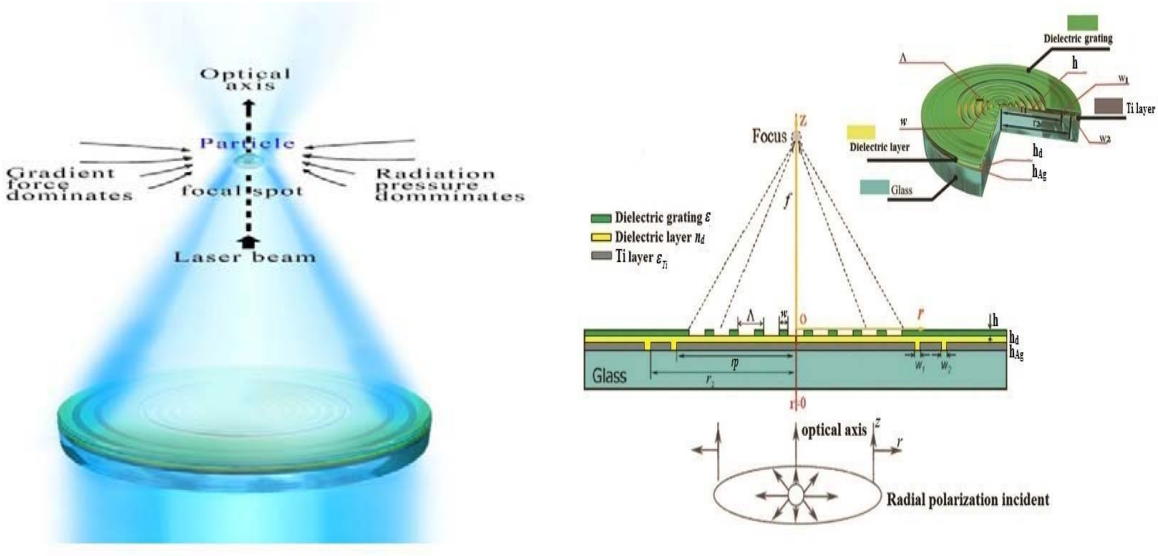

(a) (b)

Figure 1. (a) Schematic of a nanosize bead trapped by the subwavelength focus beyond the near field created by the far-field nanofocusing plasmonic lens; (b) Schematic of the far-field nanofocusing plasmonic lens in the cylindrical coordinate system is plotted as the r-z cross section, showing the geometrical parameters defining the structure, as well as the three-dimensional model is depicted at the top right corner. The $z = 0$ plane is at the glass-metal interface.

2. FAR-FIELD NANONEWTON OPTICAL FORCE TRAP STRUCTURE

Our plasmonic lens can be realized by utilizing a dielectric surface grating on the circular plasmonic lens, as shown in Fig. 1(b). The circular plasmonic lens with several slit rings ($w_{1,2} = 228\,\text{nm}$, $r_p = 2.272\,\mu\text{m}$, $r_2 = 3.395\,\mu\text{m}$) milled into titanium (Ti) film upon the glass substrate excites the cylindrical surface plasmon (CSP) waves. A dielectric layer (α-SiO_2, refractive index $n_d = 2.16$) upon the Ti film functions as a Fabry-Perot-like resonator and can enhance the focal intensity, smoothing the metallic surface and protecting the Ti thin film from sulfuration or oxidation as well. A circular dielectric grating ($\varepsilon = 2.4$, $\Lambda = 432\,\text{nm}$, $a = 202\,\text{nm}$, $h = 180\,\text{nm}$) is added topside, acting as a modulation device to extend the subwavelength focus into far field, which modulates CSP waves launched by annular Ti slits so that part of the evanescent components are coupled into the propagation waves to the far-field region to achieve nanofocusing effects by constructive interference [33, 34].

With this plasmonic lens, a subwavelength focal size of 204 nm (0.38λ) with a focal length about 2.34 μm (4.4λ) at the vacuum wavelength of 532 nm (0.35 W) has been achieved [33]. The focal length and nanoscale focal spot can be adjusted by varying the geometric parameters of this plasmonic lens [33, 34]. In addition, the far-field nanofocusing circular plasmonic lens is characterized by enhanced focusing efficiency (733%) compared with other far-field plasmonic lens. In this sense, this plasmonic lens design can help enhance trapping efficiency by high focusing efficiency to generate a strong field gradient at the focal spot area. Therefore, the trapping force can be increased without further decreasing trapping distance (near field trapping) or increasing the incident optical power, which can help avoid any physical contact with the trapped particles to prevent contamination and decrease the risk of optical damage.

However, it is very tedious to study far-field trapping behavior here by experiments only due to complex thin films coating and nanolithography processes required. Considering this, a theoretical study is carried out here first by means of computational numerical calculations for the purpose of revealing physical picture of far-field trapping behavior by using a circular plasmonic lens. The commercial software "COMSOL Multiphysics 4.3b" is adopted here for the computational calculation and numerical simulation [35–39].

3. SIMULATION RESULTS AND DISCUSSION

The incident light is the radial polarization wave with the vacuum wavelength of 532 nm (0.35 W), impinging from the bottom of the substrate. The gradient of intensity is a necessary condition for the optical traps [2, 28]. First, we calculate the intensity gradient located on the focal spot. The gradients of the electric field intensity distribution are shown in Fig. 2. The figure indicates that the maximum change rate of the electric field intensity distribution [2, 40] is located at the region of the focal spot, which means that the trapping distance approximates the focal length. Since the nanoscale focal spot can be obtained away from the lens surface, the far-field nano-optical trap may be realized.

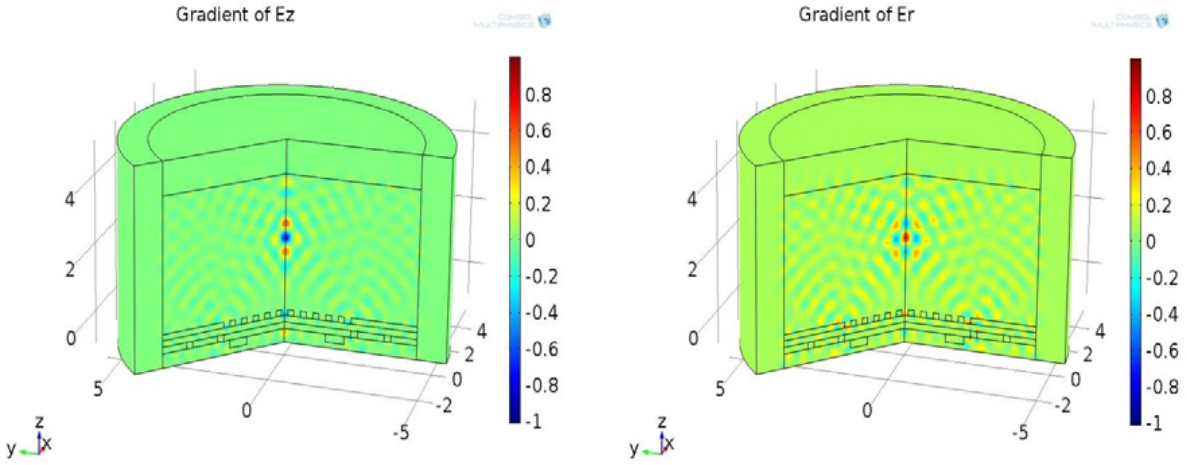

(a) (b)

Figure 2. Gradients of the electric field intensity distribution (the coordinate unit is μm): (a) The longitudinal and (b) radial distributions.

The radius of the particle is 100 nm, and its refractive index is 1.59. We note that the trapping force can be reduced by reducing the refractive index contrast between the particle and the surrounding medium by placing the particle in a medium such as water. The Maxwell's surface stress tensor (MST, $\langle T \rangle$) formalism [28, 41, 42] is used to determine the total optical force on a particle. The time averaged $\langle T \rangle$ is defined by:

$$\langle T \rangle = \frac{1}{2}\mathrm{Re}\left[\varepsilon \mathbf{E}\mathbf{E}^* + \mu \mathbf{H}\mathbf{H}^* - \frac{1}{2}\left(\varepsilon |\mathbf{E}|^2 + \mu |\mathbf{H}|^2\right) I\right] \tag{1}$$

where I denotes the identity matrix; $\mathbf{EE}^*$ and $\mathbf{HH}^*$ are the electric and magnetic fields, respectively; ε and μ are the permittivity and permeability of the surrounding medium, respectively. The components of the total time-averaged electromagnetic force F acting on the particle interacting with an optical field can be calculated using a surface integral [28]:

$$\mathbf{F} = \oint \langle T \rangle \cdot d\mathbf{S} \tag{2}$$

Thus, the total optical force on a particle can be obtained by calculating the electromagnetic fields over the bounding surface around the particle. Fig. 3(a) shows the MST over the surface enclosing the nanoparticle. As the structure rotates symmetrically and the incident light is radially polarized, we j use only a two-dimensional axis symmetry model, which is half of the cross section depicted in Fig. 1, to clearly show the MST distribution. The direction of radial MST is opposite to r-coordinate, which may push the particle toward the focal spot, while the other directions MST can be transformed to radial and longitudinal direction, respectively. These transformed radial MST is along the r direction, which will pull the particle out of the focal spot. But the transformed radial MST is weaker than the opposite radial MST. It means that the direction of resultant MST will be always opposite to r-coordinate. The transformed longitudinal MST can cause the two opposite forces at the z-coordinate. It should be noted that the opposite MST will be offset in the focal spot. In all the following cases, the nanoparticle is positioned at a certain point (r, z), and the MST method is used to calculate the forces acting on the nanoparticle at this point [39]. This process was repeated over a grid of coordinates for the nanoparticle positions to obtain the force fields. Fig. 3(b) illustrates that the particle interacts with the normalized intensity of the far-field nanofocusing circular plasmonic lens.

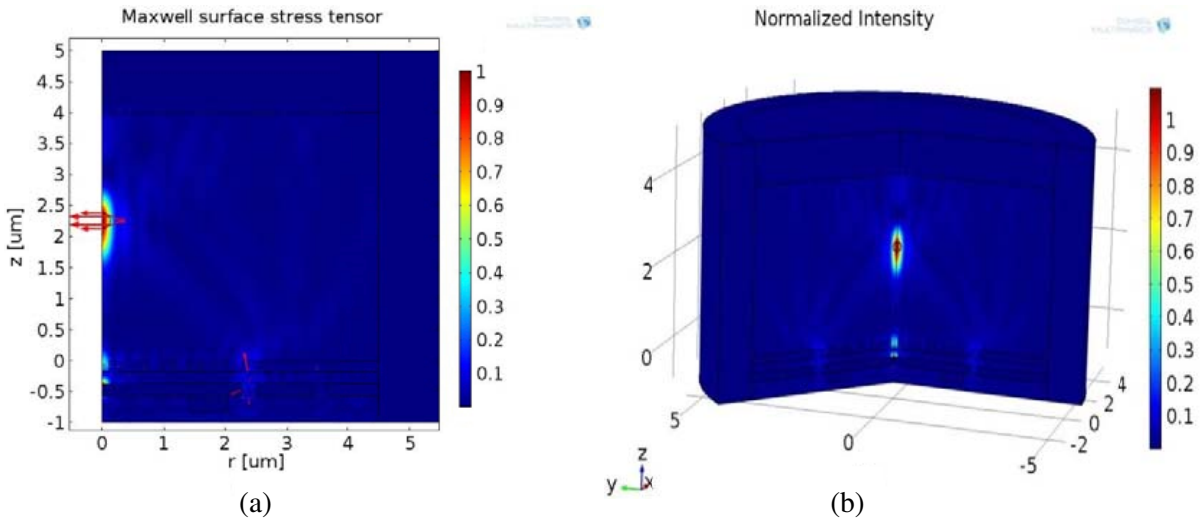

Figure 3. (a) The MST over the surface enclosing the nanoparticle; (b) interaction of the particle with the normalized intensity of the far-field nanofocusing circular plasmonic lens.

Next, we consider the optical forces generated on a nanometer-size dielectric particle interacting with this intensity distribution. The forces on the particle depend on the position of the particle in the focal spot. Figs. 4 and 5 respectively show the radial (Fr) and longitudinal (Fz) forces on a nanoparticle near the focal spot and as a function of the longitudinal and radial distance across the focal spot, respectively. Fig. 4(a) shows that a positive Fz indicates the particle pulled along the z-coordinate and that a negative Fz indicates the particle moving in the opposite direction of the z-coordinate. It should be noted that when the particle is near the focal spot, the negative force approximately equals the positive force, which may limit the particle in the focus area. The reason is that CSP can make the evanescent components coupled into the propagation waves to the far-field region to achieve nanofocusing spot by constructive interference, which causes the alternatively positive and negative stronger longitudinal gradient forces [43], as shown in Fig. 2(a) and Fig. 3(a). As a consequence, the

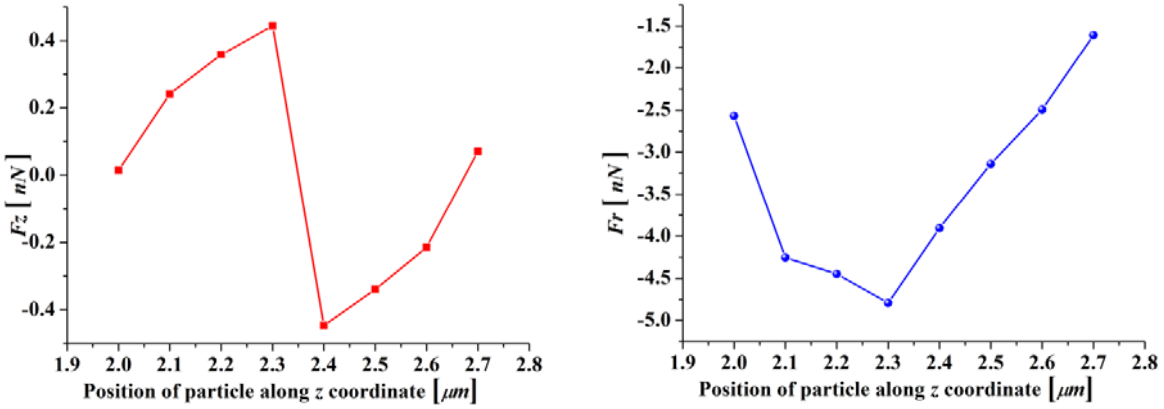

Figure 4. Radial (Fr) and longitudinal (Fz) forces on a 200 nm particle near the focal spot and as a function of longitudinal distance across the focal spot: (a) The z component of the force, (b) the r component of the force.

Fz approximates zero, and the sign of Fz will be reversed when the nanoparticle approaches the focal spot region. The r component of the force is always negative and achieves nanonewton level, as shown in Fig. 4(b). This means that there are stronger radial forces, which always push the particle to the optical axis. These results are consistent with prior results in Fig. 3.

Figure 5(a) indicates that the r component of the force gradually increases as the particle approaches the focal spot. The symmetry of the force plot is a consequence of the symmetric focal spot structure and the polarization symmetry of a radially polarized illumination. Similarly, the larger Fr is caused by the enhanced radial gradient field, as shown in Fig. 2(b) and Fig. 3(a). It should be noted that due to the high energy focusing efficiency (733%), the intensity of focal spot is much greater than that of other far-field focusing plasmonic structures [33], which means that the gradient force of focal spot will increase. In this sense, a unique plasmonic lens design can help enhance trapping efficiency by enhancing the gradient force. Therefore, trapping strength can be increased without increasing optical power or further decreasing focal size, where the maximum optical force can be calculated to be -4.76 nN near the focal spot. The trapping potential resulting from the optical forces determines the stability of the optical trap. The trapping potential (U) of a particle located at r_0 can be directly obtained from [44]:

$$U(r_0) = -\int_{\infty}^{r_0} F(r)dr \tag{3}$$

In principle, a 1 kT trapping potential well is sufficient to overcome the thermal energy of the particle and localize it in the optical trap [45] (k is Boltzmann's constant, and T is the temperature). With this design, the trapping potential of a 100 nm particle is approximately 5.57 kT by using Eq. (3), which results in a stiffer trapping potential. As noted earlier, the optical forces on Rayleigh particles are characterized by an r^3 dependence, where r is the particle radius. Therefore, the trapping potential is approximately 1 kT when the radius of particle is 56 nm, which is the smallest size that can be stably trapped by this design. This result demonstrates that the force drags the particle toward the focal spot, where transverse trapping forces are even stronger. A similar idea was implemented for optical trapping with a fiber-based surface plasmonic lens [30]. However, compared with this far-field trapping structure [30] (the force is 5.9 pN using the same dielectric nanosphere and power), our structure can achieve bigger trapping force. Interestingly, the force can be used to apply localized forces and pressures on nanoscale objects with high precision. Fig. 5(b) illustrates that the Fz lightly oscillating in the whole focal plane and Fz is very small because the negative force is approximately equal to the positive force at z-coordinate, which may remain the particle in the focus plane. Oscillations depend on the beam interference between the coupled SPP wave and diffraction wavelets generated from each ring of the circular grating.

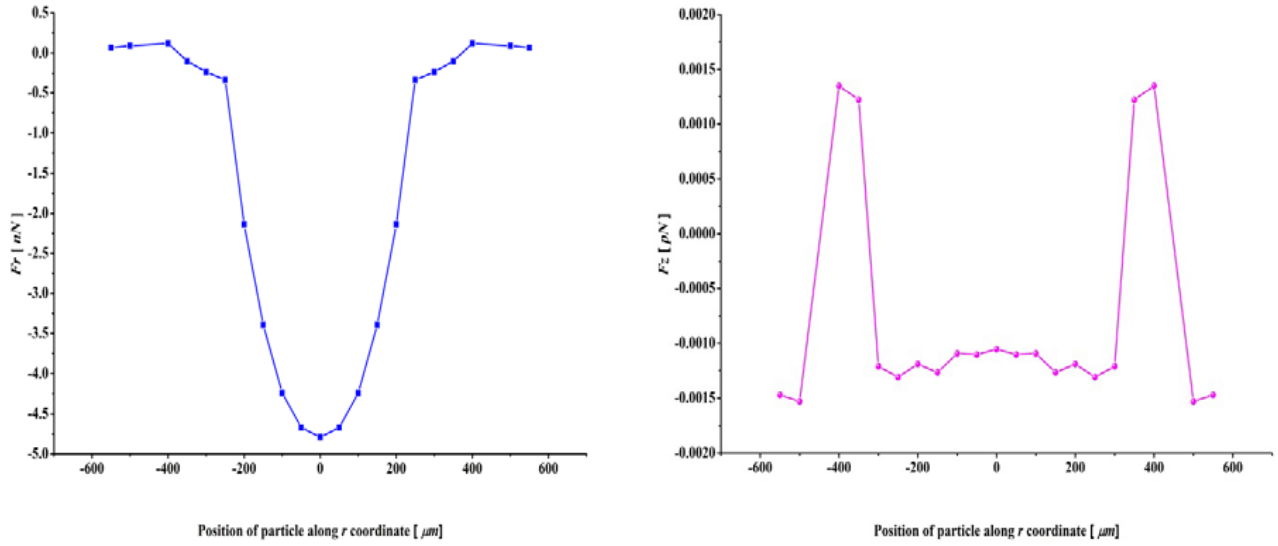

(a) (b)

Figure 5. Radial (Fr) and longitudinal (Fz) forces on a 200 nm particle near the focal spot and as a function of radial distance across the focal spot: (a) The r component of the force, (b) the z component of the force.

4. CONCLUSION

In summary, we have theoretically demonstrated the far-field nanonewton optical trapping force of subwavelength particles by using a far-field nanofocusing circular plasmonic lens. Since the far-field nanofocusing circular plasmonic lens enables high effect nanofocusing, the strong optical trapping force can be obtained. Different from the near-field traps in the vicinity of the surfaces in SP tweezers, our trap can be obtained around 4.4λ away, which can not only directly avoid any physical contact of the trapped samples to prevent contamination, but also reduce the photothermal effects associated with strong absorption of the metal nanostructures. This far-field plasmonic tweezer can not only keep all the advantages of far-field plasmonic optical tweezers, but also exhibit a stronger trapping force, which can achieve a stable 3D trap for nanosize particle by requiring low optical power. Therefore, this far-field plasmonic tweezer has great potential to become a powerful and primary tool for manipulating and sensing nanosize biological specimens.

ACKNOWLEDGMENT

The authors gratefully acknowledge the financial support from the National Natural Science Foundation of China (No. 61205204), the "Spring Sunshine" Plan (No. Z2011029), the Open Research Fund of the State Key Laboratory of Transient Optics and Photonics, Chinese Academy of Sciences (No. SKLST201107) and the Fundamental Research Funds for the Central Universities (lzujbky-2014-44).

REFERENCES

1. Ashkin, A., "Acceleration and trapping of particles by radiation pressure," *Phys. Rev. Lett.*, Vol. 24, 156–159, 1970.
2. Ashkin, A., J. M. Dziedzic, J. E. Bjorkholm, and S. Chu, "Observation of a single-beam gradient force optical trap for dielectric particles," *Opt. Lett.*, Vol. 11, 288–290, 1986.
3. Grier, D. G., "A revolution in optical manipulation," *Nature*, Vol. 424, No. 6950, 810–816, 2003.

4. Ashkin, A., "Optical trapping and manipulation of neutral particles using lasers," *Proc. Natl. Acad. Sci. U.S.A.*, Vol. 94, No. 10, 4853–4860, 1997.
5. Ashkin, A., K. Schütze, J. M. Dziedzic, U. Euteneuer, and M. Schliwa, "Force generation of organelle transport measured in vivo by an infrared laser trap," *Nature*, Vol. 348, 346–348, 1990.
6. Ukita, H., T. Saitoh, and N. Sakahara, "Resolving discrepancy between theoretical and experimental optical trapping forces using effects of beam waist and trapping position displacement due to gravity," *Opt. Rev.*, Vol. 13, No. 6, 436–442, 2006.
7. Miao, X., H. Liao, and L. Y. Lin, "Opto-plasmonic tweezers for rotation and manipulation of micro/nano objects," *Optical MEMS and Their Applications Conference, Proc. of IEEE/LEOS International Conference on IEEE*, 15–16, 2005.
8. Serey, X., S. Mandal, and D. Erickson, "Comparison of silicon photonic crystal resonator designs for optical trapping of nanomaterials," *Nanotechnology*, Vol. 21, No. 30, 305202, 2010.
9. Wang, K., E. Schonbrun, P. Steinvurzel, and K. B. Crozier, "Nanoparticle manipulation using a plasmonic nano-tweezer with an integrated heat sink," *Conference on Lasers and Electro-Optics (CLEO), OSA, QWG2*, 2011.
10. Nieto-Vesperinas, M., P. Chaumet, and A. Rahmani, "Near field photonic forces," *Phil. Trans. R. Soc. A*, Vol. 362, 719–737, 2004.
11. Erickson, D., X. Serey, Y. F. Chen, and S. Mandal, "Nanomanipulation using near field photonics," *Lab. Chip*, Vol. 11, No. 6, 995–1009, 2011.
12. Quidant, R., D. Petrov, and G. Badenes, "Radiation forces on a rayleigh dielectric sphere in a patterned optical near field," *Opt. Lett.*, Vol. 30, 1009–1011, 2005.
13. Zhang, Q., J. J. Xiao, X. M. Zhang, and Y. Yao, "Optical binding force of gold nanorod dimers coupled to a metallic slab," *Opt. Commun.*, Vols. 301–302, 121–126, 2013.
14. Lezec, H. J., A. Degiron, E. Devaux, R. A. Linke, L. Martin-Moreno, F. J. Garcia-Vidal, and T. W. Ebbesen, "Beaming light from a subwavelength aperture," *Science*, Vol. 297, No. 5582, 820–822, 2002.
15. Valdivia-Valero, F. J. and M. Nieto-Vesperinas, "Whispering gallery mode propagation in photonic crystals in front of subwavelength slit arrays: Interplay with extraordinary transmission," *Opt. Commun.*, Vol. 284, No. 7, 1726–1733, 2011.
16. Xu, H. and M. Kall, "Surface-plasmon-enhanced optical forces in silver nanoaggregates," *Phys. Rev. Lett.*, Vol. 89, No. 24, 246802–246802, 2002.
17. Arias-Gonzalez, J. R. and M. Nieto-Vesperinas, "Optical forces on small particles: Attractive and repulsive nature and plasmon-resonance conditions," *JOSA A*, Vol. 20, No. 7, 1201–1209, 2003.
18. Zelenina, A. S., R. Quidant, and M. Nieto-Vesperinas, "Enhanced optical forces between coupled resonant metal nanoparticles," *Opt. Lett.*, Vol. 32, No. 9, 1156–1158, 2007.
19. Zelenina, A. S., R. Quidant, G. Badenes, and M. Nieto-Vesperinas, "Tunable optical sorting and manipulation of nanoparticles via plasmon excitation," *Opt. Lett.*, Vol. 31, No. 13, 2054–2056, 2006.
20. Juan, M. L., M. Righini, and R. Quidant, "Plasmon nano-optical tweezers," *Nat. Photonics*, Vol. 5, No. 6, 349–356, 2011.
21. Zhang, W., L. Huang, C. Santschi, and O. J. Martin, "Trapping and sensing 10 nm metal nanoparticles using plasmonic dipole antennas," *Nano Lett.*, Vol. 10, No. 3, 1006–1011, 2010.
22. Grigorenko, A. N., N. W. Roberts, M. R. Dickinson, and Y. Zhang, "Nanometric optical tweezers based on nanostructured substrates," *Nat. Photonics*, Vol. 2, No. 6, 365–370, 2008.
23. Righini, M., A. S. Zelenina, C. Girard, and R. Quidant, "Parallel and selective trapping in a patterned plasmonic landscape," *Nat. Phys.*, Vol. 3, No. 7, 477–480, 2007.
24. Roxworthy, B. J., K. D. Ko, A. Kumar, K. H. Fung, E. K. Chow, G. L. Liu, N. X. Fang, and K. C. Toussaint, Jr., "Application of plasmonic bowtie nanoantenna arrays for optical trapping, stacking, and sorting," *Nano Lett.*, Vol. 12, No. 2, 796–801, 2012.
25. Kang, J. H., K. Kim, H. S. Ee, Y. H. Lee, T. Y. Yoon, M. K. Seo, and H. G. Park, "Low-power nano-optical vortex trapping via plasmonic diabolo nanoantennas," *Nat. Commun.*, Vol. 2, 582, 2011.

26. Righini, M., P. Ghenuche, S. Cherukulappurath, V. Myroshnychenko, F. J. García de Abajo, and R. Quidant, "Nano-optical trapping of rayleigh particles and escherichia coli bacteria with resonant optical antennas," *Nano Lett.*, Vol. 9, No. 10, 3387–3391, 2009.
27. Wang, K., E. Schonbrun, P. Steinvurzel, and K. B. Crozier, "Trapping and rotating nanoparticles using a plasmonic nano-tweezer with an integrated heat sink," *Nat. Commun.*, Vol. 2, 469, 2011.
28. Saleh, A. A. and J. A. Dionne, "Toward efficient optical trapping of sub-10-nm particles with coaxial plasmonic apertures," *Nano Lett.*, Vol. 12, No. 11, 5581–5586, 2012.
29. Garcés-Chávez, V., R. Quidant, P. J. Reece, G. Badenes, L. Torner, and K. Dholakia, "Extended organization of colloidal microparticles by surface plasmon polariton excitation," *Phys. Rev. B*, Vol. 73, No. 8, 085417, 2006.
30. Liu, Y., F. Stief, and M. Yu, "Subwavelength optical trapping with a fiber-based surface plasmonic lens," *Opt. Lett.*, Vol. 38, No. 5, 721–723, 2013.
31. Fazal, F. M. and S. M. Block, "Optical tweezers study life under tension," *Nat. Photonics*, Vol. 5, 318–321, 2011.
32. Dong, J., C. E. Castro, M. C. Boyce, M. J. Lang, and S. Lindquist, "Optical trapping with high forces reveals unexpected behaviors of prion fibrils," *Nature Struct. Mol. Biol.*, Vol. 17, 1422–1430, 2010.
33. Cheng, L., P. F. Cao, Y. Li, W. J. Kong, X. P. Zhao, and X. Zhang, "High efficient far-field nanofocusingwith tunable focus under radial polarization illumination," *Plasmonics*, Vol. 7, No. 1, 175–184, 2012.
34. Cao, P., L. Cheng, X. Zhang, W.-P. Lu, W.-J. Kong, and X.-W. Liang, "Far-field tunable nano-focusing based on metallic slits surrounded with nonlinear-variant widths and linear-variant depths of circular dielectric grating," *Progress In Electromagnetics Research*, Vol. 138, 647–660, 2013.
35. Evans, K., "Nanocrystal-based optoelectronic devices in plamonic nanojunctions," Doctoral dissertation, Masters Thesis, Rice University, 2013.
36. Roels, J., I. de Vlaminck, L. Lagae, B. Maes, D. van Thourhout, and R. Baets, "Tunable optical forces between nanophotonic waveguides," *Nature Nanotech.*, Vol. 4, No. 8, 510–513, 2009.
37. Yang, X., Y. Liu, R. F. Oulton, X. Yin, and X. Zhang, "Optical forces in hybrid plasmonic waveguides," *Nano Lett.*, Vol. 11, No. 2, 321–328, 2011.
38. Zhang, J., K. F. MacDonald, and N. I. Zheludev, "Optical gecko toe: Optically controlled attractive near-field forces between plasmonic metamaterials and dielectric or metal surfaces," *Phys. Rev. B*, Vol. 85, No. 20, 205123, 2012.
39. Ploschner, M., M. Mazilu, T. F. Krauss, and K. Dholakia, "Optical forces near a nanoantenna," *J. Nanophotonics*, Vol. 4, No. 1, 041570–041570, 2010.
40. Padgett, M. J. and R. W. Bowman, "Optical trapping and binding," *Rep. Prog. Phys.*, Vol. 76, No. 2, 026401, 2013.
41. Stratton, J. A., *Electromagnetic Theory*, Wiley, 2007.
42. Novotny, L., "Forces in optical near-fields," *Near-field Optics and Surface Plasmon Polaritons*, S. Kawata. ed., 123–141, Springer Berlin Heidelberg, 2001.
43. Chaumet, P. C., A. Rahmani, and M. Nieto-Vesperinas, "Optical trapping and manipulation of nano-objects with an apertureless probe," *Phys. Rev. Lett.*, Vol. 88, No. 12, 123601, 2002.
44. Novotny, L., R. X. Bian, and X. S. Xie, "Theory of nanometric optical tweezers," *Phys. Rev. Lett.*, Vol. 79, No. 4, 645, 1997.
45. Yang, A. H. J., T. Lerdsuchatawanich, and D. Erickson, "Forces and transport velocities for a particle in a slot waveguide," *Nano Lett.*, Vol. 9, No. 3, 1182–1188, 2009.